



Article

Identification of Antimycobacterial Natural Products from a Library of Marine Invertebrate Extracts

Kojo Sekyi Acquah ^{1,†}, Denzil R. Beukes ^{2,*} , Ronnett Seldon ³, Audrey Jordaan ⁴, Suthananda N. Sunassee ¹ , Digby F. Warner ^{4,5,6} and David W. Gammon ^{1,*}

¹ Department of Chemistry, University of Cape Town, Cape Town 7701, South Africa; acqkoj001@myuct.ac.za (K.S.A.); snsunassee@gmail.com (S.N.S.)

² School of Pharmacy, University of the Western Cape, Bellville 7535, South Africa

³ Drug Discovery and Development Centre, Department of Chemistry, University of Cape Town, Cape Town 7700, South Africa; ronnett.seldon@uct.ac.za

⁴ SAMRC/NHLS/UCT Molecular Mycobacteriology Research Unit & DST/NRF Centre of Excellence for Biomedical TB Research, Department of Pathology, Faculty of Health Sciences, University of Cape Town, Cape Town 7925, South Africa; audrey.jordaan@uct.ac.za (A.J.); digby.warner@uct.ac.za (D.F.W.)

⁵ Institute of Infectious Disease and Molecular Medicine, Faculty of Health Sciences, University of Cape Town, Cape Town 7925, South Africa

⁶ Wellcome Centre for Infectious Diseases Research in Africa, University of Cape Town, Cape Town 7701, South Africa

* Correspondence: dbeukes@uwc.ac.za (D.R.B.); david.gammon@uct.ac.za (D.W.G.)

† Current address: Division of Medicinal Chemistry, Department of Pharmaceutical Sciences, University of Connecticut, Storrs, CT 06269, USA.



Citation: Acquah, K.S.; Beukes, D.R.; Seldon, R.; Jordaan, A.; Sunassee, S.N.; Warner, D.F.; Gammon, D.W. Identification of Antimycobacterial Natural Products from a Library of Marine Invertebrate Extracts. *Medicines* **2022**, *9*, 9. <https://doi.org/10.3390/medicines9020009>

Academic Editor: Helen D. Skaltsa

Received: 24 December 2021

Accepted: 24 January 2022

Published: 28 January 2022

Publisher's Note: MDPI stays neutral with regard to jurisdictional claims in published maps and institutional affiliations.



Copyright: © 2022 by the authors. Licensee MDPI, Basel, Switzerland. This article is an open access article distributed under the terms and conditions of the Creative Commons Attribution (CC BY) license (<https://creativecommons.org/licenses/by/4.0/>).

Abstract: Tuberculosis (TB) remains a public health crisis, requiring the urgent identification of new anti-mycobacterial drugs. We screened several organic and aqueous marine invertebrate extracts for their in vitro inhibitory activity against the causative organism, *Mycobacterium tuberculosis*. Here, we report the results obtained for 54 marine invertebrate extracts. The chemical components of two of the extracts were dereplicated, using ¹H NMR and HR-LCMS with GNPS molecular networking, and these extracts were further subjected to an activity-guided isolation process to purify the bioactive components. *Hyrtios reticulatus* yielded heteronemin **1** and *Jaspis splendens* was found to produce the bengamide class of compounds, of which bengamides P **2** and Q **3** were isolated, while a new derivative, bengamide S **5**, was putatively identified and its structure predicted, based on the similarity of its MS/MS fragmentation pattern to those of other bengamides. The isolated bioactive metabolites and semi-pure fractions exhibited *M. tuberculosis* growth inhibitory activity, in the range <0.24 to 62.50 µg/mL. This study establishes the bengamides as potent antitubercular compounds, with the first report of whole-cell antitubercular activity of bengamides P **2** and Q **3**.

Keywords: antitubercular; drug discovery; marine natural product; molecular networking; heteronemin; bengamides

1. Introduction

Tuberculosis (TB), which is caused by *Mycobacterium tuberculosis* (Mtb), remains a leading cause of death, globally. Despite the availability of an effective anti-TB chemotherapy and a neonatal vaccine, an estimated 10 million people contracted TB and 1.4 million people died of the disease, globally, in 2019 [1]. The current standard combination therapy carries a high pill burden (up to four separate anti-TB drugs are used), long duration (minimum six months) of treatment and side effects or toxicities, owing to concomitant use of mixtures of TB drugs and non-TB drugs (for example, anti-HIV drugs) [1,2]. Furthermore, delayed diagnosis, inappropriate treatment and non-adherence has led to the emergence of multidrug-resistant (MDR) and extensively drug-resistant (XDR) Mtb strains [1,3]. Treatment of these resistant strains requires the use of non-frontline drugs, often over prolonged periods and

with associated risks, including severe side effects and high therapeutic cost [3–5]. There is, therefore, an urgent need to discover and develop new potent anti-TB drugs with reduced side effects and effectiveness over shorter periods.

Nature remains our primary source of medication, with the marine environment relatively less explored [6]. The ocean occupies over 70% of the Earth's surface and is uniquely rich in biodiversity. For their survival and existence, marine organisms, especially invertebrates, biosynthesize and secrete secondary metabolites to ward off competitors, predators and parasites [7]. These secondary metabolites have unique structural diversity, with a high degree of stereochemical complexity, and have shown a range of bioactivities, including anticancer, antioxidant, antifungal, antiviral, antibacterial, anti-TB, anti-inflammatory, antimalarial, analgesic and antinematodal properties [8,9]. Representative examples of marine-derived drugs include ziconotide, a peptide analgesic, derived from the marine cone snail *Conus magus*, and ecteinascidin-743, an alkaloid used in cancer treatment, derived from the sea squirt, *Ecteinascidia turbinata* [10,11]. Marine-natural products have promise in providing drug leads for the TB drug discovery pipeline and many anti-mycobacterial compounds, including the manzamines, halicyclamines, cyclostellamines, batzelladines and callyaerins have been isolated from marine organisms [12].

Natural product drug discovery starts with the screening of natural product extracts as the preliminary step to finding new lead compounds. As part of our continuous search for new anti-TB agents from marine invertebrates, we screened several marine-natural product extracts, obtained from the United States of America's National Cancer Institute (NCI) [13]. The whole-cell bioassay approach was employed, in preference to target-based and genetics-driven approaches, given the unknown bioactive compositions of the extracts and the well-described difficulties in ensuring whole-cell activity against *Mtb* [14]. Herein, we report the initial screening of 984 marine invertebrate extracts and the antimycobacterial activity results of 54 active extracts, with the detection and isolation of the active components of two of the extracts. The extracts of the sponges, *Hyrtios reticulatus* and *Jaspis splendens*, were among the most active (Table 1) and were subjected to activity-guided fractionation to isolate the active ingredients. Anti-mycobacterial activity in the extract from *Hyrtios reticulatus* was found to be associated with heteronemin 1, while, as expected [15], the extract from *Jaspis splendens* produced the bengamide class of compounds (see Figure 1), with antitubercular activity shown, for the first time, to be associated with bengamides P and Q (Figure 1, compounds 2 and 3), as well as other inseparable mixtures of bengamides. While other marine-derived and synthetically modified bengamides have previously been shown to be potent antitubercular agents and investigated as drug leads [16,17], to the best of our knowledge, this is the first report of antitubercular activity for bengamides P 2 and Q 3.

Table 1. Minimum inhibitory concentration (MIC₉₀ and MIC₉₉) of marine invertebrate extracts against *M. tuberculosis* H37Rv and classification to species level of the marine invertebrates with their source country.

Country	Phylum	Class	Order	Family	Genus	Species	NPID	MIC ₉₀ (µg/mL)	MIC ₉₉ (µg/mL)
Mauritius	Porifera	Demospongiae	Astrophorida	Ancorinidae	<i>Jaspis</i>	<i>splendens</i> (<i>Dorypleres</i>)	C019765	2.4	4.5
	Porifera	Demospongiae	Dictyoceratida	Thorectidae	<i>Hyrtios</i>	<i>reticulatus</i>	C019725	51.0	72.0
South Africa	Porifera	Demospongiae	Poecilosclerida	Guitarridae	<i>Guitarra</i>	<i>fimbriata indica</i>	C018520	70.0	87.0
	Porifera	Demospongiae	Hadromerida	Suberitidae	<i>Aaptos</i>	sp. 1	C018442	71.0	83.0
	Porifera	Demospongiae	Verongida	Aplysinnellidae	<i>Porphyria</i>	<i>pedunculata</i>	C018530	71.0	94.0
	Porifera	Demospongiae	Poecilosclerida	Hymedesmiidae	<i>Phorbas</i>	sp. 1	C018462	72.0	81.0

Table 1. Cont.

Country	Phylum	Class	Order	Family	Genus	Species	NPID	MIC ₉₀ (µg/mL)	MIC ₉₉ (µg/mL)
South Africa	Porifera	Demospongiae	Halichondrida	Heteroxyidae	<i>Higginsia</i>	<i>bidentifera</i>	C018466	72.0	83.0
	Porifera	Demospongiae	Halichondrida	Heteroxyidae	<i>Higginsia</i>	sp. 1	C018578	72.0	84.0
	Cnidaria	Hydrozoa	Leptothecatae	Aglaopheniidae	<i>Lytocarpia</i>	<i>formosa</i>	C018502	73.0	81.0
	Porifera	Demospongiae	Halichondrida	Halichondriidae	<i>Hymeniacion</i>	sp. 1	C018470	73.0	84.0
	Porifera	Demospongiae	Poecilosclerida	Guitarridae	<i>Guitarra</i>	<i>fimbriata indica</i>	C018458	73.0	91.0
	Chordata	Asciacea	Aplousobranchia	Didemnidae	<i>Didemnum</i>	<i>obscurum</i>	C019906	1.6	1.7
	Porifera	Demospongiae	Halichondrida	Dictyonellidae	<i>Stylissa</i>	sp. 1, n.sp.	C019904	17.0	19.4
	Cnidaria	Anthozoa	Alcyonacea	Nephtheidae	<i>Drifa</i>	sp. b (n.sp.)	C018631	41.0	52.0
	Porifera	Demospongiae	Poecilosclerida	Raspailiidae	<i>Echinodictyum</i>	sp. 1	C018566	25.1	42.8
	Mollusca	Polyplacophora	Chitonida	Acanthochitonidae	<i>Acanthochitona</i>	<i>garnoti</i>	C018637	0.5	0.63
	Porifera	Demospongiae	Poecilosclerida	Isodictyidae	<i>Isodictya</i>	sp. 2, n.sp.	C018626	18.8	6.25
	Porifera	Demospongiae	Poecilosclerida	Tedaniidae	<i>Hemitedania</i>	sp. 1	C018538	18.7	9.3
	Porifera	Demospongiae	Halichondrida	Halichondriidae	<i>Halichondria</i>	sp. 1	C018460	13.8	12.2
	Tanzania	Porifera	Demospongiae	Haplosclerida	Petrosiidae	<i>Neopetrosia</i>	<i>tuberosa</i> cf.	C015405	2.5
Porifera		Demospongiae	Haplosclerida	Phloeodictyidae	<i>Oceanapia</i>	<i>ramsayi</i>	C015331	22.0	28.0
Porifera		Demospongiae	Haplosclerida	Phloeodictyidae	<i>Oceanapia</i>	sp. 3	C015461	35.0	42.0
Porifera		Demospongiae	Poecilosclerida	Chondropsidae	<i>Chondropsis</i>	sp. 1	C015479	58.0	64.0
Chordata		Asciacea	Aplousobranchia	Polycitoridae	<i>Eudistoma</i>	<i>giganteum</i>	C015357	61.0	68.0
Porifera		Demospongiae	Dictyoceratida	Thorectidae	<i>Aplysinopsis</i>	<i>elegans</i> cf.	C015228	2.5	2.60
Mollusca		Gastropoda	Neogastropoda	Cypraeidae	<i>Cypraea</i>	<i>tigris</i>	C015272	47.9	57.9
Porifera		Demospongiae	Poecilosclerida	Podospongiidae	<i>Diacarnus</i>	<i>ardoukobae</i>	C015180	70.8	81.2
Chordata		Asciacea	Aplousobranchia	Didemnidae	<i>Lissoclinum</i>	<i>badium</i>	C018795	2.6	3.1
Porifera		Demospongiae	Dictyoceratida	Thorectidae	<i>Fascaplysinopsis</i>	sp. 2	C018781	7.9	16.5
Porifera		Demospongiae	Haplosclerida	Petrosiidae	<i>Petrosia</i> (<i>Strongylophora</i>)	<i>corticata</i>	C018743	31.0	35.0
Porifera		Demospongiae	Dictyoceratida	Dysideidae	<i>Dysidea</i>	sp. 17	C018675	32.0	36.0
Porifera		Demospongiae	Haplosclerida	Chalinidae	<i>Haliclona</i> (<i>Gellius</i>)	sp. 4	C018717	36.0	57.0
Porifera		Demospongiae	Dictyoceratida	Dysideidae	<i>Lamellodysidea</i>	<i>herbacea</i>	C018667	41.0	43.0
Papua-New Guinea	Porifera	Demospongiae	Dictyoceratida	Thorectidae	<i>Carterospongia</i>	sp. 3	C018787	48.0	70.0
	Porifera	Demospongiae	Dictyoceratida	Thorectidae	<i>Phyllospongia</i>	sp. 7	C018595	63.0	70.0
	Porifera	Demospongiae	Dictyoceratida	Thorectidae	<i>Aplysinopsis</i>	<i>elegans</i>	C018651	65.0	71.0
	Porifera	Demospongiae	Poecilosclerida	Mycalidae	<i>Mycale</i>	<i>setosa</i>	C018783	72.0	81.0
	Porifera	Demospongiae	Dictyoceratida	Spongiidae	<i>Spongia</i>	sp. 5	C018671	72.0	82.0
	Chordata	Asciacea	Aplousobranchia	Polyclinidae	<i>Synoicum</i>	<i>castellatum</i>	C018601	72.0	83.0
	Porifera	Demospongiae	Haplosclerida	Petrosiidae	<i>Neopetrosia</i>	<i>tuberosa</i> cf.	C018593	72.0	83.0
	Porifera	Demospongiae	'Lithistid'	Theonellidae	<i>Theonella</i>	sp. 7	C018729	73.0	83.0
	Porifera	Demospongiae	Dictyoceratida	Irciniidae	<i>Ircinia</i>	<i>arbuscula</i> cf.	C018773	< 0.24	0.5
	Porifera	Demospongiae	Hadromerida	Suberitidae	<i>Aaptos</i>	<i>nigra</i>	C018695	58.3	51.4
	Porifera	Demospongiae	Agelasida	Agelasidae	<i>Agelas</i>	<i>oxeata</i> cf.	C018756	0.4	0.9
	Porifera	Demospongiae	'Lithistid'	Scleritodermidae	<i>Aciculites</i>	<i>oxytota</i>	C018740	20.8	21.9
	Porifera	Demospongiae	'Lithistid'	Scleritodermidae	<i>Microscleroderma</i>	<i>herdmani</i>	C018684	23.7	30.6
	Porifera	Demospongiae	Haplosclerida	Callyspongiidae	<i>Callyspongia</i> (<i>Euplacella</i>)	<i>elongata</i> cf.	C018714	85.2	125.0
Porifera	Demospongiae	Haplosclerida	Niphatidae	<i>Pachychalina</i>	sp. 11	C018694	17.9	46.5	
Porifera	Demospongiae	Astrophorida	Thrombidae	<i>Thrombus</i>	sp. 1	C018716	20.8	42.5	
Porifera	Demospongiae	Haplosclerida	Niphatidae	<i>Niphates</i>	<i>elegans</i>	C018720	23.8	91.3	
Palau Islands	Porifera	Demospongiae	Halichondrida	Halichondriidae	<i>Topsentia</i>	<i>cavernosa</i>	C019960	71.9	78.9
	Porifera	Demospongiae	Hadromerida	Suberitidae	<i>Aaptos</i>	<i>nigra</i>	C019928	85.2	106.0
	Porifera	Demospongiae	Haplosclerida	Chalinidae	<i>Haliclona</i> (<i>Gellius</i>)	sp. 4	C020034	95.9	120.0
	Porifera	Demospongiae	Verongida	Aplysinellidae	<i>Porphyria</i>	sp. 1, n.sp.	C019898	113.0	125.0
Control				Rifampicin			0.02	0.03	

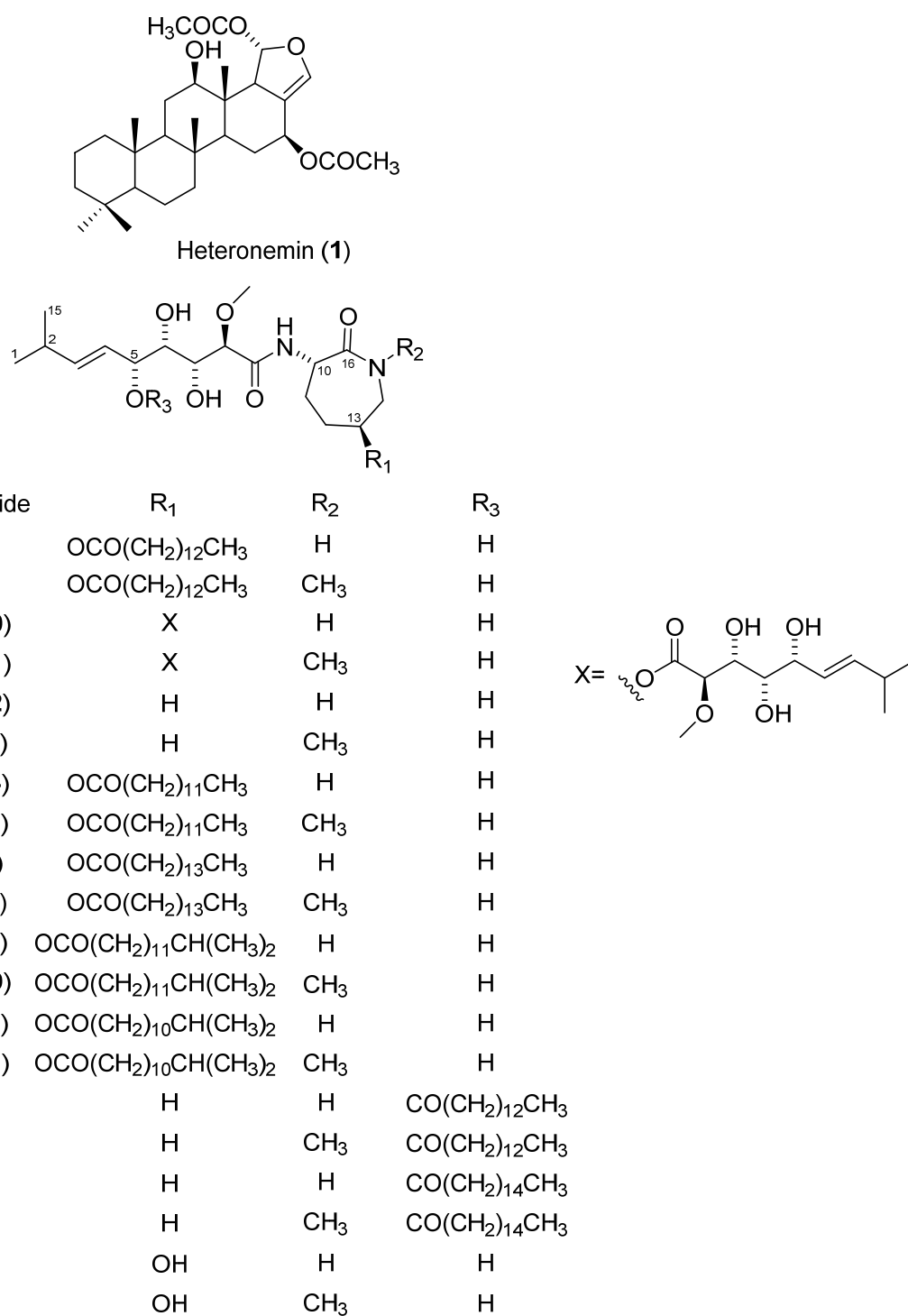


Figure 1. Structures of isolated compounds (1–3), predicted (5) and some known bengamides (4, 6–21).

2. Results and Discussion

2.1. Screening of Marine Invertebrate Samples

An initial set of 984 organic and aqueous marine invertebrate extracts were screened for their *in vitro* inhibitory activity against a fully virulent *M. tuberculosis* H37Rv fluorescent reporter mutant [16,18,19] and the minimum inhibitory concentrations required to inhibit 90% (MIC₉₀) and 99% (MIC₉₉) of the mycobacterial population were recorded. Of the 984 samples, 54 putative actives were identified and retested to confirm activity. A SciFinder® (<https://scifinder.cas.org/>, accessed on 10 February 2021) search of the species

of marine invertebrates, from which the 54 extracts were obtained, revealed that this was the first report of antimycobacterial activity in 44% of the species.

The 54 active extracts were from marine invertebrate samples, collected from the territorial waters of Mauritius (Indian Ocean) (2), South Africa (Indian and South Atlantic Oceans) (17), Tanzania (Indian Ocean) (8), Palau Island (Pacific Ocean) (4), and Papua- New Guinea (Pacific Ocean) (23). The invertebrates are of the phyla Porifera (46), Cnidaria (2), Chordata (4) and Mollusca (2). The actives displayed MIC, in the range of <0.24 to 125 µg/mL (Table 1), with 35% exhibiting good activity (MIC < 25 µg/mL), 28% moderate activity (MIC 25–65 µg/mL) and 37% weak activity (MIC 65–125 µg/mL).

The extracts of the species belonging to the genera *Jaspis*, *Didemnum*, *Acanthochitona*, *Isodictya*, *Hemitedania*, *Neopetrosia*, *Aplysinopsis*, *Cypraea*, *Lissoclinum*, *Fascaplysinopsis*, *Ircinia* and *Agelas*, exhibited the most potent activities, with sub-10 µg/mL MICs. It is worth noting that the SciFinder® search for these genera returned no reports of antimycobacterial activity, except for the genera, *Didemnum*, *Neopetrosia*, *Lissoclinum*, *Ircinia* and *Agelas*. The diterpene alkaloids, agelasines, isolated from the genus *Agelas*, and the tetracyclic bis-piperidine alkaloid, neopetrosiamine A, isolated from *Neopetrosia proxima*, as well as crude extracts of species of the genera *Didemnum*, *Lissoclinum*, *Ircinia* and *Agelas*, have been reported to show antimycobacterial activities [20–23]. This reaffirms that marine invertebrates represent a potential source of novel anti-TB compounds.

2.2. Dereplication, Molecular Networking, Isolation and Structure Elucidation

The extracts from the two Mauritian marine sponges *Hyrtios reticulatus* (SS10, MIC₉₀ = 2.40 µg/mL) and *Jaspis splendens* (SS2, MIC₉₀ = 51.00 µg/mL) were selected for preliminary investigations, in an attempt to isolate and identify the active compounds. Both extracts were available in appreciable amounts and were examples of extracts with good and moderate MIC₅₀ values, respectively. The actives were isolated using an activity-guided isolation procedure. First, the ¹H NMR spectra and HR-LCMS profiles were obtained for the bioactive extracts, and these were then subjected to bioactivity-guided fractionation, using a normal-phase solid-phase extraction (SPE) procedure, which, in each case, yielded five fractions (A–E), corresponding to polarities of the eluents. The fractions were then screened against the Mtb H37Rv reporter strain.

The HR-LCMS profile of the extract of *Hyrtios reticulatus* (SS10) showed a major peak, with *m/z* 511.3026 [M + Na]⁺, which was identified as the antimycobacterial sesquiterpene, heteronemin 1; this was confirmed by the ¹H NMR spectrum. Fractions A and B of SS10 were the most active but had the same ¹H NMR spectrum and were, therefore, combined and further purified, using normal-phase column chromatography to yield the known compound, heteronemin 1, as the most active ingredient. Heteronemin 1 was isolated as a white amorphous solid, with a molecular formula of C₂₉H₄₄O₆, deduced from HRESIMS (observed [M + Na]⁺ = 511.3026; calculated [M + Na]⁺ = 511.3036; Δ = −1.96 ppm), corresponding to eight degrees of unsaturation (Figure S1). The structure of compound 1 was fully elucidated by the analysis of HRESIMS, together with 1D and 2D NMR data, and this was congruent with that reported in the literature (Figures S1–S6 and Table S1) [24,25].

The HR-LCMS/MS data of the extract of *Jaspis splendens* (SS2) was analyzed on the GNPS molecular networking platform [26]. Dereplication of the nodes showed molecular network families, which are representative of the bengamide class of compounds; this was confirmed by the analysis of the ¹H NMR spectrum of SS2 (Figure 2, Table S4). The bengamides are a class of compounds with a core scaffold, comprising a 2(R)-methoxy-3(R),4(S),5(R)-trihydroxy-8-methylnon-6(E)-enoyl moiety, linked to an aminocaprolactam with its cyclic amide, nitrogen free or methylated [15,16,27]. Approximately 23 bengamides have been isolated, with various structural variations, enabling grouping into structural classes [16,27]. The first type contains a hydroxylysine-derived caprolactam, with the OH at C-13 either unsubstituted (bengamides Y, Z) or acylated by a lipid unit (bengamides A, B, G–J, L–O), or by polyketide esters (bengamides C, D). The second type has the lysine-derived caprolactam (which therefore does not have an OH at C-13), but with the 5-OH

acylated by the lipid unit (bengamides P–R), or not (bengamides E, E', F, F') [16,27]. Some bengamides have the same molecular formulae and weight and are only differentiated by characteristic NMR signals. For example, bengamides J and M have the same molecular formula of $C_{33}H_{60}N_2O_8$ and weight 635.4228 $[M + Na]^+$ (Figure 2, Table S3) [27].

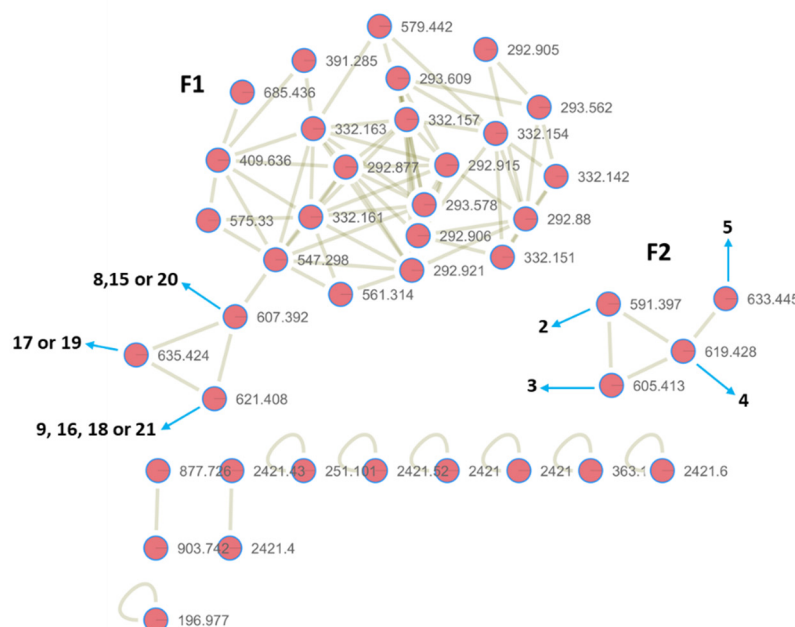


Figure 2. GNPS molecular network of the crude extract (SS2) of marine sponge *Jaspis splendens* containing some annotated nodes. Numbers in bold correspond to compounds shown in Figure 1.

Molecular cluster F1 contains the first class of bengamides with a lipid chain (Figure 2). The node with m/z 621.408 $[M + Na]^+$ corresponds to isomeric bengamides B 9, I 16, L 18 or O 21, while the node with m/z 607.392 $[M + Na]^+$ corresponds to bengamides A 8, H 15 or N 20, and the node with m/z 635.424 $[M + Na]^+$ to bengamides J 17 or M 19 (Figures 1 and 2). Family F2, which is constituted by four nodes, was dereplicated to be the second type of bengamides with a fatty acid chain, including bengamides P 2 (m/z 591.397 $[M + Na]^+$), Q 3 (m/z 605.413 $[M + Na]^+$) and R 4 (m/z 619.428 $[M + Na]^+$), which was linked to its new analogue 5 (node with m/z 633.445 $[M + Na]^+$), with a mass difference of 14 Da, signifying methylation. From the biosynthesis of bengamides and a keen examination of isolated bengamide structures, the methylation would either be on the caprolactam ring nitrogen or an elongation of the lipid chain of 4. Evaluation of the fragmentation patterns (Figure S23) of compounds 4 and 5, showed that 5 is an N-methylated analogue of 4. Compound 5 was therefore assigned the name bengamide S. Fractions B and C of SS2 exhibited the best activities, with potent MIC_{90} values of <0.24 $\mu\text{g/mL}$ and 0.25 $\mu\text{g/mL}$, respectively. The HR-LCMS profiles and ^1H NMR spectra of active fractions B and C, revealed that they comprised similar mixtures of the bengamides, and these fractions were, therefore, combined and subjected to normal-phase column chromatography. From >150 fractions collected, fractions F94 and F100 were sufficiently homogeneous for their structures to be elucidated as compounds 2 and 3, respectively. Compounds 2 and 3 had ^1H NMR signals characteristic of the second type of bengamides, with a lipid chain located as esters of the C-5 oxygen. The fact that this was attached to C-5 and not C-13 was evident from the downfield shift of the signal at δ_{H} 5.47, for the methine proton H-5 in the ^1H NMR spectrum, compared to the shielded signals for the diastereotopic C-13 methylene protons at δ_{H} 1.88 and 1.43. The structures of compounds 2 and 3 were fully elucidated by analyses of their HR-ESIMS, 1D and 2D NMR data and comparison with the literature, and confirmed to be bengamides P and Q, respectively (Figures S7–S19 and Tables S2 and S3) [27].

The ^1H NMR spectra of active fractions F107, F114 and F130 (Figures S20–S22) showed characteristic signals for bengamides of both classes with a lipid chain. However, the main component of fraction F130 was the first type of bengamide, with a branched lipid chain and characteristic upfield signals in the ^1H NMR spectrum at δ_{H} 0.7–1.7, and a signal for an N-methyl group in the caprolactam ring (δ_{H} 3.13). It is proposed that this major component may be bengamide M, as a corresponding peak of m/z 635.423 $[\text{M} + \text{Na}]^+$ was identified in the HR-LCMS profile of fraction F130.

2.3. Antimycobacterial Activity of Isolated Compounds and Semi-Pure Fractions

Heteronemin **1** exhibited an MIC_{90} of 8.23 $\mu\text{g}/\text{mL}$ against Mtb. Shown in Table 2 are the antimycobacterial activity results of isolated pure compounds and the most active semi-pure fractions obtained from purification of fractions B and C of SS2. Fraction F114 showed the greatest activity, with $\text{MIC}_{90} < 0.24 \mu\text{g}/\text{mL}$. Although bengamides have been isolated from the genus *Jaspis*, this is the first report of the detection and isolation of bengamides from *Jaspis splendens*, which is known to be a prolific producer of jasplakinolides [16].

Table 2. Minimum inhibitory concentration of bengamides P **2**, Q **3** and semi-pure fractions, obtained from purification of fractions B and C of SS2, against Mtb H37Rv, cultured for 7 and 14 days.

Compound/Fraction	MIC_{90} ($\mu\text{g}/\text{mL}$): 7 Days	MIC_{90} ($\mu\text{g}/\text{mL}$): 14 Days
2	2.14	1.03
3	62.50	31.25
F107	1.09	0.74
F114	<0.24	<0.24
F130	0.65	0.49
Rifampicin	0.02	0.01

The bengamides are potent antitumor agents, which target methionine aminopeptidase (MetAP) [15,16]. Synthetic MetAP inhibitors, based on the bengamide structural scaffold, have been described with activity against the Mtb MetAPs (the bacillus encodes two isoforms, MetAP1a and MetAP1c); however, the antimycobacterial potential (whole-cell or target-based) of natural bengamides is less explored [28,29]. There is a report of antimycobacterial activity of bengamide B **9**, which exhibited strong in vitro activity against whole-cell Mtb and the purified Mtb MetAP1C protein and was also non-toxic against human cell lines [17]. To our knowledge, ours is the first report of antimycobacterial activity for the second type of bengamides with lipid chains, namely bengamides P **2** and Q **3**. This suggests that the bengamides are potential antitubercular leads and that all known natural analogs could be screened against Mtb, to further aid in SAR and QSAR design and studies. There also appears to be value in further exploration of the Mtb MetAPs as potential drug targets.

3. Materials and Methods

3.1. General Experimental Procedure

NMR spectra were obtained on a Bruker Ascend 600 (Bruker, Billerica, MA, USA) cryoprobe prodigy at 600 MHz and 150 MHz for ^1H and ^{13}C nuclei, respectively. Chemical shifts were referenced using the corresponding undeuterated solvent signals in CD_3OD (δ_{H} 3.30, δ_{C} 47.61) and CDCl_3 (δ_{H} 7.25, δ_{C} 77.00). High-resolution mass spectrometric data were obtained using a Thermo Instrument MS system (LTQ XL/LTQ Orbitrap Discovery, Thermo Scientific, Bremen, Germany) coupled to a Thermo Instrument HPLC system (Accela PDA detector, Accela PDA autosampler and Accela pump, Thermo Scientific, Bremen, Germany). The following conditions were used: capillary voltage 45 V, capillary temperature 260 $^{\circ}\text{C}$, auxiliary gas flow rate 10–20 arbitrary units, sheath gas flow rate 40–50 arbitrary units, spray voltage 4.5 kV, mass range 100–2000 amu (maximum resolution 30,000). All solvents used throughout were HPLC-grade and purchased from both Merck and Sigma-Aldrich. Column chromatography was carried out on silica gel 60 (Fluka 70–230 mesh, 63–200 μm , Sigma-Aldrich, Buchs, Switzerland), and preparative TLC on

silica gel 60 Analtech GF254 (20 × 20 cm, 2000 µm, Analtech Inc., Newark, DE, USA). Analytical TLC was performed on Merck silica gel 60 F254 (Merck KGaA, Darmstadt, Germany) and silica gel 60 RP-18 F254 plates and bands were visualized based on the UV absorbance at 254 nm and by heating after staining with ceric ammonium sulfate reagent.

3.2. Marine Invertebrate Samples

The screening consisted of 984 organic (MeOH-CH₂Cl₂, 1:1) and aqueous (H₂O) extracts of marine invertebrate samples obtained from the National Cancer Institute (NCI), USA [13].

3.3. Antimycobacterial Activity

The crude extracts, semi-pure and isolated compounds were dissolved in DMSO and their minimum inhibition concentrations (MIC_{90/99} values) determined against the green fluorescent protein (GFP)-tagged Mtb H37Rv pMSP12:GFP bioreporter using the standard broth microdilution method developed by Collins et al. [18]. Mtb H37Rv was cultured in Middlebrook 7H9 broth medium supplemented with albumin–dextrose complex, D-glucose, and Tween-80 (7H9/ADC/Glu/Tw). The minimum concentration which inhibited the growth of 90% (MIC₉₀) or 99% (MIC₉₉) of bacilli for the tested samples was determined at 1 week and 2 weeks post-inoculation using microplate detection of GFP fluorescence intensity and expressed in µg/mL. The fluorescence was measured with excitation at 485 nm and emission at 520 nm. Growth media and 5% dimethyl sulfoxide (DMSO) were used as a negative control, with rifampicin used as a positive control.

3.4. Fractionation, Isolation and Purification of Active Compounds

The extracts SS2 and SS10 were subjected to an NCI DIOL SPE fractionation process. The organic extract (150 mg) was weighed and solubilized in 1.8 mL of 1:1 MeOH/CH₂Cl₂ and sonicated to mix. The mixture was loaded on a 2 g DIOL SPE column and eluted stepwise, with solvent mixtures of increasing polarity (a column volume/solvent mixture of 6 mL): 9:1 hexane/CH₂Cl₂ (A), 20:1 CH₂Cl₂/EtOAc (B), 100% EtOAc (C), 5:1 EtOAc:MeOH (D), 100% MeOH (E). The fractionation process was repeated with 3 × 150 mg of extract and each fraction, from A to E, was combined and dried.

Fractions A and B of SS10 were combined and further purified through a normal-phase column chromatography with an increasing polarity of a mixture of hexane/EtOAc from 1:0 hexane/EtOAc to 0:1 hexane/EtOAc to yield compound **1** (17.01 mg).

Fractions B and C of SS2 were also combined and subjected to a normal-phase column chromatography with an increasing polarity of a mixture of hexane/EtOAc from 1:0 hexane/EtOAc to 0:1 hexane/EtOAc to yield compounds **2** (3.08 mg) and **3** (0.69 mg) and a mixture of bengamides.

Heteronemin 1: white amorphous solid; for ¹H, ¹³C NMR data, see Table S1 and Figures S1–S6; HRESIMS (positive mode) *m/z* 511.3026 [M + Na]⁺ Δ −1.96 ppm; calculated for C₂₉H₄₄O₆.

Bengamide P 2: colourless oil; for ¹H, ¹³C NMR data, see Table S2 and Figures S7–S12; HRESIMS (positive mode) *m/z* 591.3978 [M + Na]⁺ Δ 2.03 ppm; calculated for C₃₁H₅₆N₂O₇.

Bengamide Q 3: colourless oil; for ¹H, ¹³C NMR data, see Table S3 and Figures S13–S19; HRESIMS (positive mode) *m/z* 605.4133 [M + Na]⁺ Δ 1.82 ppm; calculated for C₃₂H₅₈N₂O₇.

3.5. Dereplication and Molecular Networking

Raw LC–MS/MS data of sample SS2 was converted to mzXML format using the ProteoWizard tool MSconvert (version 3.0.10051, Vanderbilt University, United States) [30]. The mzXML data was uploaded to the Global Natural Products Social (GNPS) Molecular Networking (MN) webserver3 (<http://gnps.ucsd.edu>, accessed on 12 August 2020) and analyzed using the MN workflow [23]. The data was filtered by removing all MS/MS fragment ions within +/− 17 Da of the precursor *m/z*. MS/MS spectra were window filtered by choosing only the top 6 fragment ions in the +/− 50Da window throughout the spectrum. The precursor ion mass tolerance was set to 0.02 Da and a MS/MS fragment ion

tolerance of 0.02 Da. A network was then created where edges were filtered to have a cosine score above 0.7 and more than 3 matched peaks. Further, edges between two nodes were kept in the network, only if each of the nodes appeared in each other's respective top 10 most similar nodes. Finally, the maximum size of a molecular family was set to 100, and the lowest scoring edges were removed from molecular families until the molecular family size was below this threshold. The spectra in the network were then searched against GNPS' spectral libraries. The library spectra were filtered in the same manner as the input data. All matches kept between network spectra and library spectra were required to have a score above 0.7 and at least 3 matched peaks. The output of the molecular network was visualized using Cytoscape version 3.7.2 [31] and displayed using the settings "preferred layout" with "directed" style. The nodes (compounds) originating from the solvent control (MeOH) were excluded from the original network to enable visualization of only the compounds in SS2.

4. Conclusions

Marine-natural products are a reliable source of potent antitubercular leads, as this screening project identified 54 actives in whole-cell growth inhibition assays (MIC_{90} range: < 0.244–125 $\mu\text{g}/\text{mL}$). Notably, 44% of the species from which these extracts were obtained are reported here, for the first time, as possessing antimycobacterial activity. A combination of ^1H NMR and HR-LCMS dereplication, along with GNPS molecular networking and a bioactivity-guided isolation techniques was employed to detect and isolate heteronemin and the bengamides P and Q, as the respective active ingredients of the extracts of the Mauritian sponges *Hyrtios reticulatus* and *Jaspis splendens*. A new bengamide derivative was detected in the molecular network of SS2. In this study, the bengamides have been identified as potent antimycobacterial compounds and should be explored further. Moreover, the isolation of promising active compounds from crude extracts, with high and moderate activity, provides compelling evidence for the continuous need to explore the rich resource of the NCI's repository of marine invertebrate extracts further, for novel anti-TB leads.

Supplementary Materials: The following supporting information can be downloaded at: <https://www.mdpi.com/article/10.3390/medicines9020009/s1>, Figure S1: HR-ESI-MS spectrum of heteronemin 1, Figure S2: ^1H -NMR spectrum (600 MHz, CDCl_3 , 303 K) of heteronemin 1, Figure S3: ^{13}C -NMR spectrum (150 MHz, CDCl_3 , 303 K) of heteronemin 1, Figure S4: HSQC NMR spectrum (600 MHz, CDCl_3 , 303 K) of heteronemin 1, Figure S5: ^1H - ^1H COSY spectrum (600 MHz, CDCl_3 , 303 K) of heteronemin 1, Figure S6: HMBC NMR spectrum (600 MHz, CDCl_3 , 303 K) of heteronemin 1, Figure S7: HR-ESI-MS spectrum of bengamide P 2, Figure S8: ^1H -NMR spectrum (600 MHz, CDCl_3 , 303 K) of bengamide P 2, Figure S9: ^{13}C -NMR spectrum (150 MHz, CDCl_3 , 303 K) of bengamide P 2, Figure S10: ^1H - ^1H COSY spectrum (600 MHz, CDCl_3 , 303 K) of bengamide P 2, Figure S11: HSQC NMR spectrum (600 MHz, CDCl_3 , 303 K) of bengamide P 2, Figure S12: HMBC NMR spectrum (600 MHz, CDCl_3 , 303 K) of bengamide P 2, Figure S13: HR-ESI-MS spectrum of bengamide Q 3, Figure S14: ^1H -NMR spectrum (600 MHz, CDCl_3 , 303 K) of bengamide Q 3, Figure S15: ^{13}C -NMR spectrum (150 MHz, CDCl_3 , 303 K) of bengamide Q 3, Figure S16: HSQC NMR spectrum (600 MHz, CDCl_3 , 303 K) of bengamide Q 3, Figure S17: ^1H - ^1H COSY spectrum (600 MHz, CDCl_3 , 303 K) of bengamide Q 3, Figure S18: ^1H - ^1H TOCSY spectrum (600 MHz, CDCl_3 , 303 K) of bengamide Q 3, Figure S19: HMBC NMR spectrum (600 MHz, CDCl_3 , 303 K) of bengamide Q 3, Figure S20: ^1H -NMR spectrum (600 MHz, CDCl_3 , 303 K) of F107, Figure S21: ^1H -NMR spectrum (600 MHz, CDCl_3 , 303 K) of F114, Figure S22: ^1H -NMR spectrum (600 MHz, CDCl_3 , 303 K) of F130, Figure S23: MS/MS fragmentation pattern of bengamide R 4 (A) and bengamide S 5 (B) with fragment ions circled in red showing methylation is on the nitrogen of the caprolactam ring, Table S1: ^{13}C and ^1H chemical shifts of Heteronemin 1 isolated and that reported in literature, Table S2: ^{13}C and ^1H chemical shifts of bengamide P 2 isolated and that reported in literature, Table S3: ^{13}C and ^1H chemical shifts of bengamide Q 3 isolated and that reported in literature, Table S4: Compounds isolated and tentatively identified in the molecular cluster of the crude extract (SS2) of the sponge *Jaspis splendens* with their corresponding masses (observed and calculated), molecular formulae (MF), and mass error (ID (Δ ppm)).

Author Contributions: Conceptualization, D.R.B., S.N.S. and D.W.G.; Data curation, R.S. and A.J.; Formal analysis, K.S.A.; Funding acquisition, S.N.S.; Investigation, K.S.A., D.F.W. and D.W.G.;

Methodology, K.S.A., D.R.B., R.S., A.J. and D.F.W.; Project administration, D.W.G.; Resources, S.N.S. and D.W.G.; Supervision, D.R.B., S.N.S., D.F.W. and D.W.G.; Validation, A.J.; Writing—original draft, K.S.A.; Writing—review & editing, D.R.B., S.N.S., D.F.W. and D.W.G. All authors have read and agreed to the published version of the manuscript.

Funding: This work was partly supported by a grant from the South African National Research Foundation to DRB (Grant No. 118569). D.F.W. acknowledges the financial support of the South African National Research Foundation (NRF), the Strategic Health Innovation Partnerships (SHIP) Unit of the South African Medical Research Council, with funds received from the South African Department of Science Innovation, and the Research Council of Norway (R&D Project 261669 “Reversing antimicrobial resistance”). S.N.S. acknowledges funding from the South African National Research Foundation (NRF), the Newton Advanced Fellowship Award (NA160057) and the American Society of Pharmacognosy (ASP) Research Starter Grant. K.S.A. also acknowledges funding from the University of Cape Town.

Institutional Review Board Statement: Not applicable.

Informed Consent Statement: Not applicable.

Data Availability Statement: Not applicable.

Acknowledgments: David Newman (formerly) and Barry O’Keefe, from The Natural Products Branch, Developmental Therapeutics Program, National Cancer Institute, National Institutes of Health (USA), is gratefully acknowledged for providing the screening library. We also acknowledge the Marine Biodiscovery Centre, Department of Chemistry, University of Aberdeen for LCMS experiments.

Conflicts of Interest: The authors declare no conflict of interest. The funders had no role in the design of the study, in the collection, analyses, interpretation of data, in the writing of the manuscript, or in the decision to publish the results.

References

1. WHO. *Global Tuberculosis Report*; WHO: Geneva, Switzerland, 2020.
2. Snell, N.J.C. The treatment of tuberculosis: Current status and future prospects. *Expert Opin. Investig. Drugs* **1998**, *7*, 545–552. [[CrossRef](#)] [[PubMed](#)]
3. Nguta, J.M.; Appiah-Opong, R.; Nyarko, A.K.; Yeboah-Manu, D.; Addo, P.G.A. Current perspectives in drug discovery against tuberculosis from natural products. *Int. J. Mycobacteriol.* **2015**, *4*, 165–183. [[CrossRef](#)] [[PubMed](#)]
4. Riccardi, G.; Pasca, M.R. Trends in discovery of new drugs for tuberculosis therapy. *J. Antibiot.* **2014**, *67*, 655–659. [[CrossRef](#)] [[PubMed](#)]
5. Blanco, D.; Perez-Herran, E.; Cacho, M.; Ballell, L.; Castro, J.; Del Río, R.G.; Lavandera, J.L.; Remuiñán, M.J.; Richards, C.; Rullas, J.; et al. Mycobacterium tuberculosis Gyrase Inhibitors as a New Class of Antitubercular Drugs. *Antimicrob. Agents Chemother.* **2015**, *59*, 1868–1875. [[CrossRef](#)] [[PubMed](#)]
6. Cragg, G.M.; Newman, D.J. Natural products: A continuing source of novel drug leads. *Biochim. Biophys. Acta* **2013**, *1830*, 3670–3695. [[CrossRef](#)] [[PubMed](#)]
7. Paul, V.J.; Ritson-Williams, R. Marine chemical ecology. *Nat. Prod. Rep.* **2008**, *25*, 662–695. [[CrossRef](#)] [[PubMed](#)]
8. Patridge, E.; Gareiss, P.; Kinch, M.S.; Hoyer, D. natural products and their derivatives. *Drug Discov. Today* **2016**, *21*, 204–207. [[CrossRef](#)]
9. Gerwick, W.H.; Moore, B.S. Lessons from the past and charting the future of marine natural products drug discovery and chemical biology. *Chem. Biol.* **2013**, *19*, 85–98. [[CrossRef](#)]
10. Bowersox, S.S.; Luther, R. Pharmacotherapeutic potential of Omega-Conotoxin MVIIA (SNX-111), an N-type neuronal calcium channel blocker found in the venom of *Conus magus*. *Toxicon* **1998**, *36*, 1651–1658. [[CrossRef](#)]
11. Rinehart, K.L.; Holt, T.G.; Fregeau, N.L.; Stroh, J.G.; Keifer, P.A.; Sun, F.; Li, L.H.; Martin, D.G. Ecteinascidins 729, 743, 745, 759A, 759B, and 770: Potent antitumor agents from the Caribbean tunicate *Ecteinascidia turbinata*. *J. Org. Chem.* **1990**, *55*, 4512–4515. [[CrossRef](#)]
12. Hou, X.; Wang, C.; Gerwick, W.H.; Shao, C. European Journal of Medicinal Chemistry Marine natural products as potential anti-tubercular agents. *Eur. J. Med. Chem.* **2019**, *165*, 273–292. [[CrossRef](#)] [[PubMed](#)]
13. Thornburg, C.C.; Britt, J.R.; Evans, J.R.; Akee, R.K.; Whitt, J.A.; Trinh, S.K.; Harris, M.J.; Thompson, J.R.; Ewing, T.L.; Shipley, S.M.; et al. NCI Program for Natural Product Discovery: A Publicly-Accessible Library of Natural Product Fractions for High-Throughput Screening. *ACS Chem. Biol.* **2018**, *13*, 2484–2497. [[CrossRef](#)] [[PubMed](#)]
14. Sass, P. Postgenomic strategies in antibacterial drug discovery. *Futur. Microbiol* **2010**, *5*, 1553–1579.
15. White, K.N.; Tenney, K.; Crews, P. The Bengamides: A Mini-Review of Natural Sources, Analogues, Biological Properties, Biosynthetic Origins, and Future Prospects. *J. Nat. Prod.* **2017**, *80*, 740–755. [[CrossRef](#)] [[PubMed](#)]

16. Garcí, C.; Sarabia, F. Chemistry and Biology of Bengamides and Bengazoles, Bioactive Natural Products from Jaspis Sponges. *Mar. Drugs* **2014**, *12*, 1580–1622. [[CrossRef](#)]
17. Quan, D.H.; Nagalingam, G.; Luck, I.; Proschogo, N.; Pillalamarri, V.; Addlagatta, A.; Martinez, E.; Sintchenko, V.; Rutledge, P.J.; Triccas, J.A. Bengamides display potent activity against drug-resistant *Mycobacterium tuberculosis*. *Sci. Rep.* **2019**, *9*, 14396. [[CrossRef](#)]
18. Collins, L.A.; Torrero, M.N.; Franzblau, S.G. Green Fluorescent Protein Reporter Microplate Assay for High-Throughput Screening of Compounds against *Mycobacterium tuberculosis*. *Antimicrob. Agents Chemother.* **1998**, *42*, 344–347. [[CrossRef](#)]
19. Abrahams, G.L.; Kumar, A.; Savvi, S.; Hung, A.W.; Wen, S.; Abell, C.; Barry, E.C.; Sherman, D.R.; Boshoff, H.I.; Mizrahi, V. Pathway-selective sensitization of *Mycobacterium tuberculosis* for target-based whole-cell screening. *Chem. Biol.* **2013**, *19*, 844–854. [[CrossRef](#)]
20. Selegim, M.H.R.; Lira, S.P.; Kossuga, M.H.; Batista, T.; Berlinck, R.G.S.; Hajdu, E.; Muricy, G.; da Rocha, R.M.; do Nascimento, G.G.F.; Silva, M.; et al. Antibiotic, cytotoxic and enzyme inhibitory activity of crude extracts from Brazilian marine invertebrates. *Braz. J. Pharmacogn.* **2007**, *17*, 287–318. [[CrossRef](#)]
21. Wei, X.; Karinel, N.R.A.D. Neopetrosiamine A, biologically active bis-piperidine alkaloid from the Caribbean Sea sponge *Neopetrosia proxima*. *Bioorg. Med. Chem. Lett.* **2010**, *20*, 5905–5908. [[CrossRef](#)]
22. Arai, M.; Yamano, Y.; Setiawan, A.; Kobayashi, M. Identification of the Target Protein of Agelasine D, a Marine Sponge Diterpene Alkaloid, as an Anti-dormant *Mycobacterial* Substance. *Chem. Bio. Chem.* **2014**, *35145*, 117–123. [[CrossRef](#)] [[PubMed](#)]
23. Mangalindan, G.C.; Talaue, M.T.; Cruz, L.J.; Franzblau, S.G.; Concepcion, G.P.; Adams, L.B.; Richardson, A.D.; Ireland, C.M. Agelasine F from a Philippine *Agelas* sp. Sponge Exhibits in vitro Antituberculosis Activity. *Planta Med.* **2000**, *66*, 364–365. [[CrossRef](#)] [[PubMed](#)]
24. Kazlauskas, R.; Murphy, P.T.; Quinn, R.J.; Wells, R.J. Heteronemin, A new Scalarin type Sesterterpene from the sponge *Heteronema erecta*. *Tetrahedron Lett.* **1976**, *17*, 2631–2634. [[CrossRef](#)]
25. Bourguet-Kondracki, M.L.; Martin, M.T.; Debitus, C.; Guyot, M. 12-epi-Heteronemin: New Sesterterpene From Sponge the marine sponge *Hyrtilis erecta*. *Tetrahedron Lett.* **1994**, *35*, 109–110. [[CrossRef](#)]
26. Networking, S.M. Perspective Sharing and community curation of mass spectrometry data with Global Natural Products Social Molecular Networking. *Nat. Biotechnol.* **2016**, *34*, 828–837.
27. Thale, Z.; Kinder, F.R.; Bair, K.W.; Bontempo, J.; Czuchta, A.M.; Versace, R.W.; Phillips, P.E.; Sanders, M.L.; Wattanasin, S.; Crews, P. Bengamides revisited: New structures and antitumor studies. *J. Org. Chem.* **2001**, *66*, 1733–1741. [[CrossRef](#)]
28. Lu, J.; Yuan, X.; Yuan, H.; Wang, W.; Wan, B.; Franzblau, S.G.; Ye, Q. Inhibition of *Mycobacterium tuberculosis* methionine aminopeptidases by bengamide derivatives. *Chem. Med. Chem.* **2012**, *6*, 1041–1048. [[CrossRef](#)]
29. Lu, J.; Yuan, X.; Ye, Q. Structural analysis of inhibition of *Mycobacterium tuberculosis* methionine aminopeptidase by bengamide derivatives. *Eur. J. Med. Chem.* **2012**, *47*, 479–484. [[CrossRef](#)]
30. Holman, J.D.; Tabb, D.L.; Mallick, P. Employing ProteoWizard to Convert Raw Mass Spectrometry Data. *Curr. Protoc. Bioinform.* **2015**, *46*, 918–920. [[CrossRef](#)]
31. Otasek, D.; Morris, J.H.; Bouças, J.; Pico, A.R.; Demchak, B. Cytoscape Automation: Empowering workflow-based network analysis. *Genome Biol.* **2019**, *20*, 185. [[CrossRef](#)]